

# A complex adaptive systems approach to the kinetic folding of RNA

Wilfred Ndifon

Departments of Biology and Mathematics,  
Morgan State University, Baltimore, MD 21251  
windi1@mymail.morgan.edu

July 20, 2005

## Abstract

The kinetic folding of RNA sequences into secondary structures is modeled as a complex adaptive system, the components of which are possible RNA structural rearrangements (SRs) and their associated bases and base pairs. RNA bases and base pairs engage in local stacking interactions that determine the probabilities (or fitnesses) of possible SRs. Meanwhile, selection operates at the level of SRs; an autonomous stochastic process periodically (i.e., from one time step to another) selects a subset of possible SRs for realization based on the fitnesses of the SRs. Using examples based on selected natural and synthetic RNAs, the model is shown to qualitatively reproduce characteristic (nonlinear) RNA folding dynamics such as the attainment by RNAs of alternative stable states. Possible applications of the model to the analysis of properties of fitness landscapes, and of the RNA sequence to structure mapping are discussed.

## 1 Introduction

RNA takes part in a variety of important cellular activities, including protein synthesis, intron splicing, gene silencing, and genome rearrangement (Lee et al., 2002; Mochizuki et al., 2002; Gratias & Betermier, 2003; Yang et al.,

2003). Considering the extensive functional repertoire of RNA molecules, it is of interest to determine their (functional) native structures and to understand the (kinetic) process by which they fold into such structures. The native structures of RNA molecules can be computed efficiently, at the functionally relevant secondary structure level, using free-energy minimization methods (Hofacker et al., 1994; Mathews et al., 2004) or, in cases where sufficient homologous sequences are available, by phylogenetic comparisons (Woese & Pace, 1993; Cannone et al., 2002).

Several algorithms have been developed for studying the kinetic process by which RNA molecules fold into their native secondary (Mironov & Kister, 1985; Morgan & Higgs, 1996; Flamm et al., 2000; Zhang & Chen, 2000; Wolfinger et al., 2003; Tang et al., 2004; Ndifon & Nkwanta, 2005) and tertiary (Abrahams et al., 1990; Gulyaev et al., 1990; Isambert, 2000; Xayaphoumine et al., 2003) structures. The majority of these algorithms (e.g., see Isambert, 2000; Xayaphoumine et al., 2003; Ndifon & Nkwanta, 2005) operate on a helix-based move-set, involving the formation and dissociation of entire RNA helices. On the other hand, a few of the algorithms (e.g., see Zhang & Chen, 2000; Wolfinger et al., 2003) operate on a pair-based move-set; they model the RNA folding process as a time-series of structural transitions, involving the formation and dissociation of individual RNA base pairs.

Flamm and colleagues (Flamm, 1998; Flamm et al., 2000) have extended the afore-mentioned pair-based move-set by introducing the concept of base pair *shifting*, which makes possible description of the biological process of defect-diffusion, believed to be an important feature of the *in vivo* folding kinetics of RNA (Poerschke, 1974a). The folding model developed in this paper implements this extended pair-based move-set and is inspired by the theory of complex adaptive systems (see Section 3). The applicability of the model is illustrated through several examples based on selected natural and synthetic RNAs (see Section 4). In particular, the folding kinetics of the

yeast tRNA<sup>Phe</sup> is shown to be strongly influenced by modifications to specific hairpin loops. In addition, a characteristic optimal folding temperature  $T_{opt}$  ( $\approx 313K$ ) of tRNA<sup>Phe</sup>, at which the native state exhibits maximal accessibility, is identified. Furthermore, estimates are obtained for the population dynamics of two alternative stable states of SV11, an RNA species that is replicated by  $Q\beta$  replicase (Zamora et al., 1995).

The remainder of this paper is organized as follows. In Section 2, we present some concepts related to RNA secondary structures and folding kinetics. We introduce the theory of complex adaptive systems and discuss details of the new folding model in Section 3. In Section 4, we apply the model to some example problems and discuss other possible applications in Section 5.

## 2 Background information

### 2.1 RNA secondary structure

Let  $X$  be an arbitrary RNA sequence of length  $n$ . We think of  $X$  as a string  $X = x_1x_2\cdots x_n$  defined over the nucleotide alphabet  $\{A, C, G, U\}$ . The nucleotides or bases of  $X$  have a propensity to *pair* (or form canonical and non-canonical bonds) with each other. A pair formed by the bases  $x_i$  and  $x_j$ ,  $i < j$ , is denoted by  $(i, j)$ . Two base pairs  $(i, j)$  and  $(i', j')$  are said to be compatible if either  $i < i' < j' < j$  or  $i < j < i' < j'$ . If we let  $H$  be the set of possible pairs that can be formed by the bases of  $X$ , then a secondary structure  $S$  of  $X$  can be thought of as a set of mutually compatible base pairs drawn from  $H$ . The multiset consisting of all subsets of  $H$ , including the empty set (i.e., the open chain), forms the conformation space of  $X$ , denoted here by  $\zeta(X)$ . Note that incompatible base pairs form pseudoknots, which are prohibited from occurring in the folding model developed in this paper. The model can, however, be readily extended to allow the formation of pseudoknots once reliable thermodynamic parameters for such tertiary

structural elements become available.

## 2.2 Kinetic folding

The kinetic folding of an RNA sequence  $X$  at the coarse-grained secondary structure level can be thought of as a time-series of structural transitions, mediated by a set of operations called the move-set (Flamm, 1998). Each operation or *move* converts one secondary structure  $S_i \in \zeta(X)$  into another  $S_j \in \zeta(X)$ . For each structure  $S_i \in \zeta(X)$ , the move-set defines a neighborhood  $N(S_i)$  such that  $S_j \in \zeta(X)$  belongs to  $N(S_i)$  if and only if  $d(S_i, S_j) \leq d \in \mathbb{R}^+$ , where  $d(S_i, S_j)$  is the (Hamming) distance between structures  $S_i$  and  $S_j$  and  $d$  is the "move distance". Only *moves* that convert  $S_i$  into some  $S_j \in N(S_i)$  are legal. The probability of a legal move is given by a rate equation, an example of which is the Metropolis rule (Metropolis et al., 1953):

$$k_{ij} = \begin{cases} e^{\frac{-(G_j - G_i)}{RT}}, & \text{if } G_j < G_i \\ 1, & \text{if } G_j \geq G_i \end{cases} \quad (1)$$

where  $P(S_i \rightarrow S_j)$  is the probability of converting  $S_i$  into  $S_j \in N(S_i)$  by a single *move*;  $G_i$  and  $G_j$  are, respectively, the free energies of  $S_i$  and  $S_j$ , computed using a suitable choice of free-energy parameters (e.g., Mathews et al., 1999).

Conventional Monte Carlo RNA folding algorithms execute in each time step  $t + \delta t$  a *move* that converts the nascent RNA structure  $S_t$  into some structure  $S_{t+\delta t}$ , where  $S_t$  denotes the secondary structure of  $X$  at time  $t$ . The time-ordered series of structures  $\{S_t\}_{t \geq 0}$ , with  $S_t \in \zeta(X)$  and  $S_{t=0}$  the open chain, is called a folding trajectory of  $X$ . The folding time  $\tau_f$  associated with a given folding trajectory is the minimum value of  $t$  for which  $S_t$  is the native structure of  $X$ . A folding trajectory satisfying the following condition is called a folding path (Flamm et al., 2000):  $S_{t_1} = S_{t_2}$  if and only if  $t_1 = t_2$ .

## 3 The RNA folding model

### 3.1 Complex adaptive systems

The RNA folding model presented below is inspired by basic ideas from the theory of complex adaptive systems. Specifically, a complex adaptive system (CAS) is characterized by the presence of a diverse ensemble of components that engage in local interactions and an autonomous process that selects a subset of those components for enhancement based on the results of the local interactions (Levin, 1998). From these component-level dynamics emerge important global (i.e., system-level) properties such as self-organization and nonlinearity. Self-organization refers to the emergence of order from local interactions between the components of a CAS. Self-organization tends to drive a CAS towards stable configurations or states. In addition, a CAS exhibits nonlinearity; the rules that govern local interactions between the components of a CAS change as the CAS evolves (Levin, 1998). Consequently, a CAS may evolve along any one of a multitude of trajectories and may attain alternative stable states (Levin, 1998), depending on its particular evolutionary trajectory. See Levin (1998) and the references therein for further information on CASs.

### 3.2 Details of the model

The kinetic folding of RNA sequences into secondary structures is viewed here as a time-series of structural rearrangements (SRs), involving the formation, dissociation, and *shifting* of individual RNA base pairs. It is modeled as a hierarchically-structured CAS; at the lowest level of the hierarchy are RNA bases and base pairs that engage in local stacking interactions. The results of these stacking interactions determine the probabilities (or fitnesses) of possible SRs. These probabilities are given by

$$P_f^{(i,j)} = e^{-\frac{\Delta G^{ij}}{2RT}}, \quad (2)$$

$$P_d^{(i,j)} = \frac{1}{P_f^{(i,j)}}, \text{ and} \quad (3)$$

$$P_s^{(i,j) \rightarrow (i,k)} = P_d^{(i,j)} P_f^{(i,k)}, \quad (4)$$

where  $P_f^{(i,j)}$ ,  $P_d^{(i,j)}$ , and  $P_s^{(i,j) \rightarrow (i,k)}$  are, respectively, the probabilities of formation and dissociation of  $(i, j)$ , and of *shifting*  $(i, j)$  into  $(i, k)$ ,  $R$  is the gas constant,  $T$  is the absolute temperature, and  $\Delta G^{ij}$  is the stacking (including single-base stacking) energy associated with  $(i, j)$ . For an isolated base pair  $(i, j)$ ,

$$\Delta G^{ij} = \Delta G^{rij} + c \ln(j - i), c \geq 0, \quad (5)$$

Equation (5) takes into account the entropy of a loop of size  $(j - i)$ . A suitable value for the parameter  $c$  is 1.75 (Fisher, 1966). Stacking energy calculations are based on the Turner 3.1 energy rules (Mathews et al., 1999), at temperature  $T = 310.5K$ , and on the Turner 2.3 energy rules (Freier et al., 1986), at other temperatures. Equations (2), (3), (4) are based on the Kawasaki dynamics (1966); here, the dynamics involve transitions between states associated with specific local contexts of an RNA secondary structure.

The next level of the hierarchical structure is occupied by SRs. It is at this level that selection operates. An autonomous stochastic sampling process (Baker, 1987) periodically (i.e., from one time step to another) selects a subset of possible SRs for realization based on the fitnesses of the SRs. The ensemble of possible SRs changes from one time step to another thereby assuring its diversity (see below). Note that due to the inter-dependence of local stacking interactions, on which the fitnesses of SRs depend, it is necessary to ensure that the SRs that are selected for realization in the same time step be mutually independent. Therefore if there is an SR involving the base  $x_i$ , then no other SR that involves the nearest-neighbor bases and base pairs of  $x_i$  can occur in the same time step. Furthermore, in order to prevent the formation of pseudoknots SRs may only involve accessible bases;

two bases  $x_i$  and  $x_j$ ,  $i < j$ , are accessible if for  $k = i + 1, \dots, j - 1$  there is no base pair  $(k, l)$  (resp.  $(l, k)$ ) such that  $l > j$  (resp.  $l < i$ ).

To understand the model just described, consider the kinetic folding of an RNA sequence  $X$ . Denote by  $\mathfrak{R}$  the set of possible SRs that are available for realization in a given time step.  $\mathfrak{R}$  will contain as many elements as there are structures in  $N(S_t)$ , where  $S_t$  is the nascent structure of  $X$ . Each element of  $\mathfrak{R}$  is associated with specific bases and base pairs that belong to that element's "local context". For instance, an SR that involves the formation of the base pair  $(i, j)$  is associated with  $(i, j)$  and all nearest-neighbor bases and base pairs of  $(i, j)$ . Stacking interactions between the bases and base pairs associated with a given SR determine that SR's probability or fitness. This fitness is used periodically by an autonomous stochastic process to select a subset of SRs from  $\mathfrak{R}$  for realization.

As SRs are realized (and removed from  $\mathfrak{R}$ ), existing SRs may become impractical while new SRs may become possible. For instance, the formation of  $(i, j)$  in a given time step may make possible the *shifting* of  $(i, j)$  into some  $(i, k)$  in the next time step. Conversely, the dissociation of  $(i, j)$  in a given time step will render impractical the *shifting* of  $(i, j)$  into some other base pair in the next time step. New SRs that become possible are added to  $\mathfrak{R}$  while those that become impractical are removed from  $\mathfrak{R}$ . This assures the diversity of possible SRs. Note that the idea that the selective enhancement of components (i.e., SRs in this case) of a given system leads to their removal (or elimination) as well as the elimination of other components from that system appears to be at odds with what takes place in most known CASs. In the present case, the goal of selection is to, indirectly, enhance the thermal stabilities of the local contexts associated with SRs.

We note here that the inter-dependence of local stacking interactions, on which the fitnesses of SRs depend, implies that a given SR may "interact" with many other SRs. For instance, an SR that involves the base pair  $(i, j)$  will "interact" with all SRs that involve either of the bases  $x_i$  and  $x_j$ . This

implies a relatively high average degree of "epistatic" interactions between SRs. Results from studies based on random Boolean networks predict that such a high degree of epistasis leads to rugged fitness landscapes with numerous attractors (Kauffman and Levin, 1987; Kauffman, 1989). This prediction is consistent with the well-known rugged nature of RNA folding energy landscapes.

We further note that SRs, as defined in the model, operate at much more local scales of space than is the case with most existing folding methods (e.g., see Flamm et al., 2000; Isambert et. al., 2000; Tang et al., 2004). The fitnesses of SRs depend exclusively on the stacking energies associated with specific local contexts of the nascent RNA structure,  $S_t$ , and not on the free-energies of structures found in  $N(S_t)$ . Therefore, there is no need for explicit computation of the free-energies of RNA structures in the present model, in contrast to, e.g., the folding method of Flamm et al. (2000). We expect the model to reproduce global characteristics of CASs such as self-organization and nonlinearity. In particular, RNA molecules are "self-organizing" since, through their own internal dynamics, they tend to fold into thermodynamically favorable or stable states. Folding RNA molecules also exhibit nonlinear dynamics, as evinced by their attainment of alternative stable states. In Section 4, we will illustrate such nonlinear dynamics using an example based on SV11.

### 3.3 Computer implementation of the model

The above model has been implemented in the computer program *kfold*, which is available from the author upon request. For an input RNA sequence of length  $n$ , the program selects  $m = 1$  SR, if  $n \leq 30$ , and  $m = 7$  SRs, if  $n > 30$ , for realization in each time step. The folding time is incremented in each time step by the reciprocal of the product of  $m$  and the sum of the fitnesses of all possible SRs. The number of selected SRs  $m$  can be adjusted by the user. Note that the choice of  $m$  influences the computer time required



to fold an input RNA sequence but has minimal effect on the qualitative folding kinetics of the sequence (see example in Table 1). Also note that in order to speed up folding simulations, the program currently only allows the formation of base pairs that can be stacked. Specifically, a base pair  $(i, j)$  can be stacked if there exists complementary bases  $x_l$  and  $x_k$ ,  $l < k$ , such that either  $i - k = l - j = 1$  or  $k - i = j - l = 1$ .

$m$	Time steps	Fraction of A	Fraction of B
1	249	0.40	0.60
3	89	0.41	0.59
5	134	0.38	0.62
7	169	0.42	0.58
9	241	0.45	0.55
11	> 30000	0.40	0.60

Table 1. Influence of  $m$  on folding kinetics for the sequence

*GUCCUUGCGUGAGGACAGCCCUUAUGUGAGGGC*,

with  $n = 33$ . It was folded with (((((((((((((((.....)))))))))))))) (A) and ((((((.....)))))).(((((((.....))))))) (B) serving as target structures. The fraction of simulations that found either structure within the allowed time scale (i.e.,  $4 \times 10^4$  time steps) is similar for different values of  $m$ . On the other hand, the number of time steps, which reflects the amount of computer time required for folding, decreases as  $m$  increases from 1 to 3, and subsequently increases with  $m$ . 50% of simulations failed to find either target structure for  $m = 11$ . The number of time steps given for  $m = 11$  thus represents a lower bound of its actual value. Note that each data point was averaged from just 500 folding simulations run at  $T = 310.5K$ . Therefore, there may be errors in the data resulting from limited sampling of possible folding trajectories.

## 4 Example applications

We now use the new folding model, as implemented in *kfold*, to study the effects of base modifications and temperature on the folding kinetics of the yeast tRNA<sup>Phe</sup>. We also estimate the population dynamics of two alternative stable states of the synthetic SV11. These examples will demonstrate that the folding model qualitatively reproduces characteristic RNA folding dynamics. Note that in the following examples, the folding times (i.e., mean first passage times) were scaled using experimentally measured folding times (in  $\mu s$ ) of the hairpin *AAAAAACCCCCCUUUUUU* (Poerschke, 1974b). This was done in order to allow direct comparisons with folding times reported in Flamm (1998). Unless otherwise noted, all folding simulations were run at  $T = 310.5K$ .

### 4.1 Influence of base modifications on folding kinetics

A number of tRNA sequences are known to contain base modifications. Such modifications, believed to be the consequence of evolutionary optimization, have been shown to improve the foldabilities of some tRNAs (Flamm, 1998; Flamm et al., 2000). We have introduced several base modifications to the individual hairpins of the yeast tRNA<sup>Phe</sup> sequence and studied the folding kinetics of the modified sequences. All modified bases were prohibited from engaging in bond formation and stacking interactions. The modified sequences are shown in Table 2.

Sequence	Modified Hairpins	Modified Sequence Positions
<i>seq1</i>	1, 2 & 3	15, 17, 19, 37, 38, 55, 56 & 59
<i>seq2</i>	1 & 2	15, 17, 19, 37 & 38
<i>seq3</i>	1 & 3	15, 17, 19, 55, 56 & 59
<i>seq4</i>	2 & 3	37, 38, 55, 56 & 59
<i>seq5</i>	<i>None</i>	<i>None</i>

Table 2. Modified tRNA sequences used in this example. Note that hairpins are labeled from left to right, with "1" representing the left-most hairpin.

We found base modifications to elicit substantial improvements in tRNA foldabilities, in the form of drastic decreases in folding times (see Figure 1). For the unmodified sequence, *seq5*, the fraction of folded sequences (i.e., sequences that have found the native cloverleaf structure) increased relatively slowly, reaching about 45% after the first 600 $\mu s$ , and 100% within 4500 $\mu s$ . For all modified sequences, on the other hand, the fraction of folded sequences increased rapidly, reaching 100% within 1500 $\mu s$ . Among these sequences, *seq1* was the fastest folder with an estimated folding time of 300 $\mu s$ , while *seq4* was the slowest folder with a folding time of 1500 $\mu s$ . The folding times of *seq2* and *seq3* were approximately equal (i.e., about 800 $\mu s$ ). These observed effects of base modifications on tRNA folding kinetics are consistent with experimental data, as well as with predictions made by *kinfold* (Flamm, 1998). Note that we were able to simulate much longer folding times for tRNA<sup>Phe</sup>, up to 4500 $\mu s$ , than was done in Flamm (1998).

## 4.2 Temperature dependence of folding kinetics

We have used the folding model to study the temperature dependence of the folding time  $\tau_f$  of the yeast tRNA<sup>Phe</sup>. We found a V-shaped temperature dependence of  $\tau_f$  (see Figure 2), suggesting the existence of an optimal folding temperature  $T_{opt} \approx 313K$ . A possible explanation for the existence of  $T_{opt}$  is as follows: At temperatures  $T > T_{opt}$ , there are numerous structures with similar free-energies as the native cloverleaf. The native cloverleaf is therefore relatively unstable at temperatures above  $T_{opt}$  and may be associated with a much smaller basin of attraction in the energy landscape. It therefore takes the folding tRNA longer to "find" the cloverleaf among the ensemble of nonnative states. On the other hand, at temperatures  $T < T_{opt}$ , the stability of nonnative structures increases leading to a growth in the

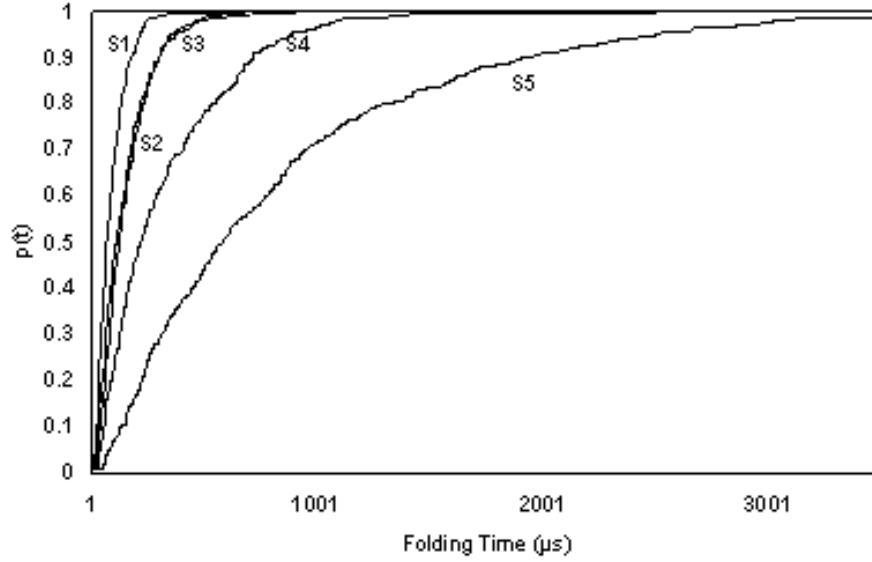


Figure 1: Folding kinetics of modified tRNA sequences (see Table 2). For each sequence, 1000 *kfold* simulations were run for  $1 \times 10^4 \mu s$  or until the native cloverleaf was found.  $p(t)$  denotes the fraction of simulations that found the cloverleaf within  $t \mu s$ . Note that the displayed folding times may not be biologically realistic as they were scaled using the folding kinetics of a hairpin. Further calibration with experimental data is necessary in order to ensure biological relevance of the displayed time scales.

number and, perhaps, sizes of nonnative basins of attraction in the energy landscape. These nonnative basins of attraction may decrease the folding tRNA’s chances of finding the native state. Both scenarios (i.e.,  $T > T_{opt}$  and  $T < T_{opt}$ ) lead to suboptimal native state accessibilities. Meanwhile, the maximal accessibility of the native state that is evident at  $T = T_{opt}$  suggests the existence at  $T_{opt}$  of optimal balance between the thermal stabilities of native and nonnative states. Note that  $T_{opt}$  is close to the optimal growth temperature range for many yeast species. Detailed analysis of the temperature dependence of folding kinetics for tRNAs and other functional RNAs from various organisms will allow us to determine if this observation is a consequence of evolutionary optimization or simply a chance occurrence.

### 4.3 (Meta)stable states

During kinetic folding, some RNA molecules may get trapped in long-lived, nonnative states called metastable states/conformations. Examples of such metastable RNA molecules include riboswitches that regulate gene expression in bacteria by switching between alternative stable conformations (Vitreschack et al., 2004). By adopting a repressing conformation, a riboswitch can elicit the premature termination of DNA transcription or the inhibition of protein translation. Detailed *in silico* analysis of the folding kinetics of a metastable RNA molecule can provide insight into its functionality. For instance, Nagel et al. (1999) used computer simulations to identify a metastable structure of the *Hok* mRNA that mediates apoptosis in plasmid R1-free cells. The predictions made by their simulations were in good agreement with experimental data (Nagel, 1999). See Higgs (2000) for other examples of how computer simulations have yielded important insight into the folding kinetics of metastable RNA molecules.

SV11 is a 115nt synthetic RNA species that exists in two alternative stable states, a rod-like stable conformation and a multi-component metastable conformation (see Figure 3). While the metastable conformation is a tem-

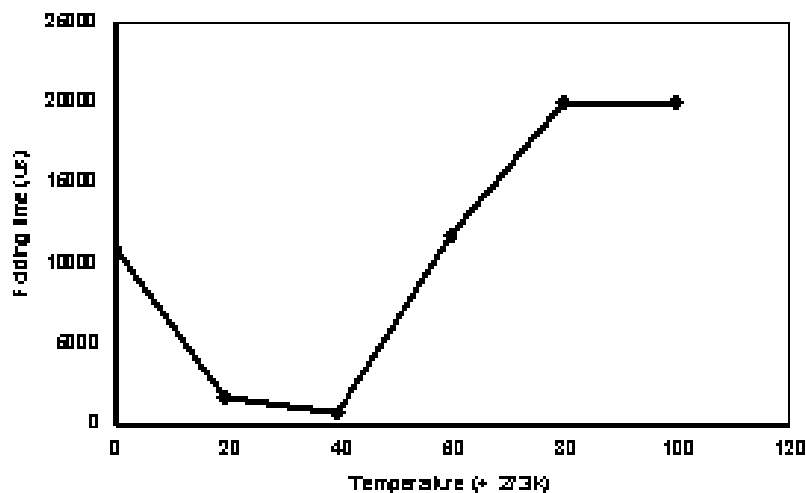


Figure 2: Temperature dependence of the folding time for tRNA obtained from folding simulations run at  $T = 273, 293, 313, 333, 353$ , and  $373K$ . None of the simulations found the ground state at  $T = 353$  and  $373K$  within  $2 \times 10^4 \mu s$ . The folding times shown for these temperatures therefore represent lower-bounds of their actual values. Energy calculations were based on the Turner 2.3 energy parameters (Freier et al., 1986), for which extrapolations to temperatures other than  $310.5K$  are readily available. Each data point was averaged from just 500 folding simulations. Therefore, there may be errors in the data resulting from limited sampling of possible folding trajectories.

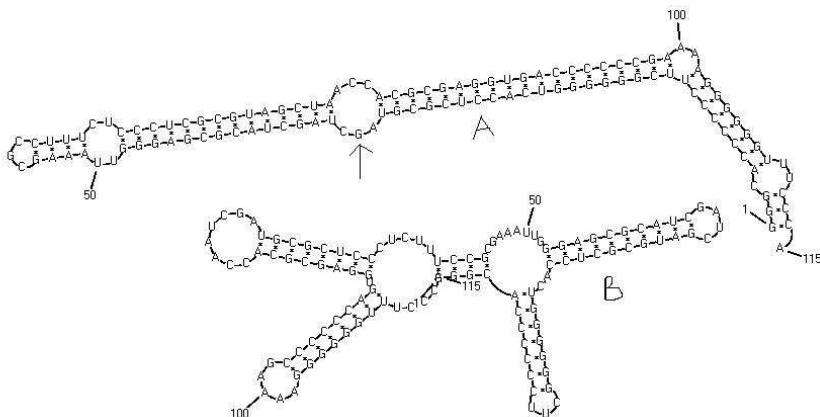


Figure 3: The stable (A) and metastable (B) structures of SV11. Note that a 33GC79 base pair (see arrow) was removed from the stable structure since *kfold* currently only allows base pairs that can be stacked; there are no complementary bases  $x_l$  and  $x_k$ ,  $l < k$ , in the SV11 sequence such that either  $33 - k = l - 79 = 1$  or  $k - 33 = 79 - l = 1$ .

plate for Q $\beta$  replicase, the stable conformation is not (Zamora et al., 1995). Several authors have previously performed *in silico* analysis of the folding kinetics of SV11. Some of the authors (Flamm, 1998; Flamm et al., 2000) successfully predicted the existence of the metastable conformation while others (e.g., see Gultyaev et al., 1990; Morgan & Higgs, 1996) could only do so if folding was constrained to occur in conjunction with transcription. However, none of the authors obtained detailed theoretical estimates of the population dynamics of the molecule’s two alternative stable states.

Here we report detailed estimates of the population dynamics of the stable and metastable conformations of SV11. As shown in Figure 4 the population of the metastable state increases steadily, reaching a maximum after about  $2000\mu s$ . In experiments performed using *kinfold*, Flamm (1998) reported that the fraction of the metastable state reached about 16% after  $500\mu s$ . This estimate is consistent with the results shown in Figure 4. However, we were able to fold the molecule for much longer, up to  $1.5 \times 10^4\mu s$ , than was done in

Flamm (1998). This allowed us to estimate the population dynamics of not just the metastable conformation but also of the stable native conformation. The ratio of the fraction of simulations that found the native conformation to the fraction that found the metastable conformation in the time scale of the simulation was approximately 3 to 1. Note that the accuracy of these results can be tested directly, in the laboratory.

## 5 Discussion

In this paper, we introduced a new model for the kinetic folding of RNA sequences into secondary structures that was inspired by the theory of complex adaptive systems. In the folding model, RNA bases and base pairs engage in local stacking interactions that determine the probabilities (or fitnesses) of possible RNA structural rearrangements (SRs). Meanwhile, selection operates at the level of SRs; an autonomous stochastic sampling process periodically selects a subset of possible SRs for realization based on the fitnesses of the SRs. Several examples were used to illustrate the applicability of the model. In particular, certain base modifications were shown to substantially improve the foldability of tRNA<sup>Phe</sup>. In addition, a characteristic optimal folding temperature  $T_{opt}$  ( $\approx 313K$ ) of tRNA<sup>Phe</sup> was identified. Furthermore, the model was used to confirm previous experimental results (Zamora et al., 1995) regarding the existence of two alternative stable states of the Q $\beta$  variant SV11, and to obtain (experimentally verifiable) estimates of the population dynamics of those states. The above examples demonstrated, among other things, the emergence from (local) SRs of nonlinear RNA folding dynamics (i.e., the realization of alternative stable states). Other possible applications of the model are discussed below.

The analysis of properties of fitness landscapes is currently of interest to researchers in a wide range of fields including the life, computer, and social sciences (e.g., see Hadany & Beker, 2003; McCarthy, 2004; Skellett



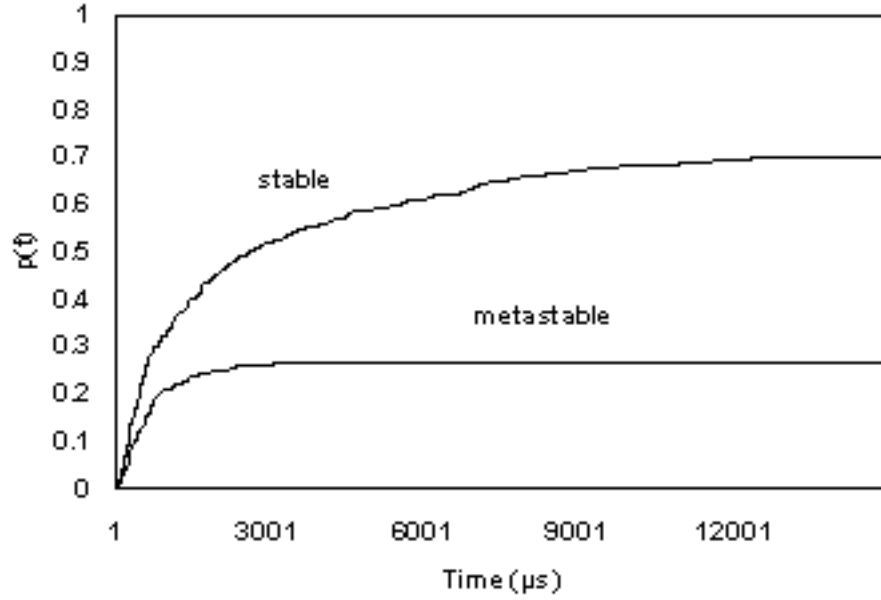


Figure 4: Folding kinetics of SV11, obtained from 1000 *kfold* simulations. Each simulation was stopped after it found either of the molecule’s two alternative stable states.  $p(t)$  denotes the fraction of simulations that found either state within  $t\mu s$ . Note that the displayed folding times may not be biologically realistic as they were scaled using the folding kinetics of a hairpin. Further calibration with experimental data is necessary in order to ensure biological relevance of the displayed time scales.

et al., 2005). A number of interesting general features of these landscapes such as positive correlations between the degree of epistasis, the number of local optima, and the expected value of the global optimum have thus far been elucidated in the context of adaptive walks on landscapes generated by random Boolean networks (RBNs) (Kauffman & Levin, 1987; Kauffman, 1989; Skellett et al., 2005) . The simplicity of RBNs and their accessibility to some degree of mathematical analysis make them convenient for use as generators of fitness landscapes. However, some of the general properties of such RBN-generated landscapes may differ from those of landscapes found in Nature. RNA folding kinetics, as modeled in this paper, could serve as a generator of, and therefore assist the analysis of properties of "natural" fitness landscapes (i.e., RNA folding energy landscapes). Note that this proposed use of RNA in the investigation of fitness landscapes differs from the previous related use of the RNA sequence to structure mapping (Schuster & Stadler, 1994), which was not based on folding kinetics.

The model could also be used to study the RNA sequence to structure (or genotype to phenotype) mapping, from a kinetics perspective. Previous investigations, based on the thermodynamics of RNA folding, have made several important findings about the RNA sequence to structure mapping such as the existence of (1) extended neutral networks of sequences that fold into the same secondary structures (2) few common or "typical" structures, realized with relatively high frequencies, and (3) many rare structures that have little or no evolutionary significance (Schuster et al., 1994; Schuster et al., 1998). These findings, together with results from thermodynamics-based RNA optimization experiments (Fontana & Schuster, 1998), have confirmed previous hypotheses on, and shed light into several important features of the process of molecular evolution, including the role of neutrality in adaptation and the existence of continuous/discontinuous transitions or punctuated equilibria in evolutionary trajectories. It would be interesting to determine how the nature of the RNA sequence to structure mapping, as obtained from

thermodynamic folding experiments, changes when RNA folding kinetics is taken into account. It is also possible that an investigation of the genotype to phenotype mapping based on the kinetics of RNA folding will yield further insight into the process of molecular evolution.

## 6 Acknowledgements

This work was funded in part by DOE-ER63580 and by RCMI Grant no. RR017581. The author thanks Dr. Asamoah Nkwanta and anonymous reviewers for their useful comments on an earlier version of the manuscript.

## 7 References

- Abrahams, J.P., van den Berg, M., van Batenburg, E., Pleij, C, 1990. Prediction of RNA secondary structure, including pseudoknotting, by computer simulation. *Nucl. Acids Res.* 18, 3035-3044.
- Baker, J. E., 1987. Reducing bias and inefficiency in the selection algorithm. In: Grefenstette, E. (Ed.), *Proceedings of the Second International Conference on Genetic Algorithms and their Application*. Lawrence Erlbaum Associates, Hillsdale, pp. 14-21.
- Cannone, J.J., Subramanian, S., Schnare, M.N., Collett, J.R., D’Souza, L.M., Du, Y., Feng, B., Lin, N., Madabusi, L.V., Muller, K.M., Pande, N., Shang, Z., Yu, N., and Gutell, R.R., 2002. The comparative RNA web (CRW) site: an online database of comparative sequence and structure information for ribosomal, intron, and other RNAs. *BMC Bioinformatics* 3, 2.
- Fisher, M.E., 1966. Effect of excluded volume on phase transitions in biopolymers. *J. Chem. Phys.* 45, 1469–1473.

- Flamm, C., 1998. Kinetic folding of RNA. Doctoral dissertation. University of Vienna, Austria.
- Flamm, C., Fontana, W., Hofacker, I.L., Schuster, P., 2000. RNA folding at elementary step resolution. *RNA* 6, 325-338.
- Fontana, W., Schuster, P., 1998. Continuity in evolution: On the nature of transitions. *Science* 280, 1451-1455.
- Freier, S.M., Kierzek, R., Jaeger, J.A., Sugimoto, N., Caruthers, M.H., Neilson, T., Turner, D.H. 1986. Improved parameters for predictions of RNA RNA duplex stability. *Proc. Natl. Acad. Sci.* 83, 9373-9377.
- Gratias, A., Betermier, M., 2003. Processing of double-strand breaks is involved in the precise excision of paramecium internal eliminated sequences. *Mol. Cell. Biol.* 7152-7162.
- Gulyaev, A.P., van Batenburg, F.H.D., Pleij, C.W.A., 1995. The influence of a metastable structure in plasmid primer RNA on antisense RNA binding kinetics. *Nucl. Acids Res.* 23, 3718-3725.
- Gulyaev, A.P., van Batenburg, F.H.D., Pleij, C.W.A., 1990. The computer simulation of RNA folding pathways using a genetic algorithm. *J. Mol. Biol.*, 250, 37-51.
- Hadany, L., Beker, T., 2003. Fitness-associated recombination on rugged adaptive landscapes. *J. Evol. Biol.* 16, 862-870.
- Higgs, P.G., 2000. RNA secondary structure: physical and computational aspects. *Quat. Rev. Biophys.* 33, 199-253.
- Hofacker, I.L, Fontana, W., Stadler, P.F., Bonhoffer, S., Tacker, M., Schuster, P., 1994. Fast folding and comparison of RNA secondary structures. *Monatsch. Chem.* 125, 167-188.

- Isambert, H., Siggia, E.D., 2000. Modeling RNA folding paths with pseudoknots: application to hepatitis delta virus ribozyme. *Proc. Natl. Acad. Sci.* 97, 6515-6520.
- Kawasaki, K., 1966. Diffusion constants near the critical point for time-dependent Ising models. *Phys. Rev.* 145, 224-230.
- Kauffman, S.A., 1989. Adaptation on rugged landscapes. In D. Stein (ed.) *Lectures in the Sciences of Complexity*, lecture volume 1, pp. 527-618. Addison-Wesley, Redwood City.
- Kauffman, S.A., Levin, S.A., 1987. Towards a general theory of adaptive walks on rugged landscapes. *J. Theor. Biol.* 128, 11-45.
- Lee, N.S., Dohjima, T., Bauer, G., Li, H., Li, M.J., Ehsani, A., Salvaterra, P., Rossi, J., 2002. Expression of small interfering RNAs targeted against HIV-1 rev transcripts in human cells. *Nat. Biotechnol.* 20, 500-505.
- Levin, S.A., 1998. Ecosystems and the biosphere as complex adaptive systems. *Ecosystems* 1, 431-436.
- Mathews, D.H., Sabina, J., Zuker, M., Turner, D.H., 1999. Expanded sequence dependence of thermodynamic parameters provides robust prediction of RNA secondary structure. *J. Mol. Biol.* 288, 911-940.
- Mathews, D.H., Disney, M.D., Childs, J.L., Schroeder, S.J., Zuker, M., Turner, D.H., 2004. Incorporating chemical modification constraints into a dynamic programming algorithm for prediction of RNA secondary structure. *Proc. Natl. Acad. Sci.* 101, 7287-7292.
- McCarthy, I.P., 2004. Manufacturing strategy: understanding the fitness landscape. *Intl. J. Op. Prod. Mgt.* 24, 124-150.

- Metropolis, N., Rosenbluth, A. W., Rosenbluth, M. N., Teller, A. H., Teller, E., 1953. Equation of state calculations by fast computing machines. *J. Chem. Phys.* 21, 1087–1092.
- Mironov, A., Kister, A., 1985. A kinetic approach to the prediction of RNA secondary structures. *J. Biomol. Struct. Dyn.* 2, 953–962.
- Mochizuki, K., Fine N.A., Fujisawa T., Gorovsky, M.A., 2002. Analysis of a piwi-related gene implicates small RNAs in genome rearrangement in *Tetrahymena*. *Cell* 110, 689–699.
- Morgan, S.R., Higgs, P.G., 1996. Evidence for kinetic effects in the folding of large RNA molecules. *J. Chem. Phys.* 105, 7152–7157.
- Nagel, J.H.A., Gultyaev, A.P., Gerdes, K., Pleij, C.W.A., 1999. Metastable structures and refolding kinetics in hok mRNA of plasmid R1. *RNA* 5, 1408–1419.
- Ndifon, W., Nkwanta, A., 2005. An agent-oriented simulation of RNA folding and its application to the analysis of RNA conformational spaces. In: Yilmaz, L. (Ed.), *Proceedings of the Agent-Directed Simulation Symposium of the 2005 Spring Simulation Multiconference*, SCS Press, San Diego, pp. 198–204.
- Poerschke, D., 1974a. Model calculations on the kinetics of oligonucleotide double helix coil transitions. Evidence for a fast chain sliding reaction. *Biophys. Chem.* 2, 83–96.
- Poerschke, D., 1974b. Thermodynamic and kinetic parameters of an oligonucleotide hairpin helix. *Biophys. Chem.* 1, 381–386.
- Schuster, P., Fontana, W., Stadler, P., Hofacker, I.L., 1994. From sequences to shapes and back: A case study in RNA secondary structures. *Proc. Roy. Soc. (London) B* 255, 279–284.

- Schuster, P., Fontana, W., 1998. Chance and necessity: Lessons from RNA. *Physica D* 133, 427-452.
- Schuster, P., Stadler, P., 1994. Landscapes: complex optimization problems and biopolymer structure. *Comput. Chem.* 18, 295-314.
- Skellett, B., Cairns, B., Geard, N., Tonkes, B., Wiles, J., 2005. Maximally rugged NK landscapes contain the highest peaks. In: Beyer, H.G., O'Reilley, U.M., Arnold, D.V., et al. (Eds.), *Proceedings of the 2005 Genetic and Evolutionary Computation Conference*, ACM Press, New York, pp. 579-584.
- Tang, X., Kirkpatrick, B., Thomas, S., Song, G., Amato, N., 2004. Using motion planning to study RNA folding kinetics. In *Proceedings of the International Conference on Computational Molecular Biology (RECOMB)*. ACM Press, San Diego, pp. 252-261.
- Vitreschack, A.G., Rodinov, D.A., Mironov, A.A., Gelfand, M.S., 2004. Riboswitches: the oldest mechanism for the regulation of gene expression? *Trends Genet.* 20, 44-50.
- Woese, C.R., Pace, N.R., 1993. Probing RNA structure, function, and history by comparative analysis. In: Gesteland, R.F., Atkins, J.F. (Eds.), *The RNA World*. Cold Spring Harbor Laboratory Press, New York, pp. 91-117.
- Wolfinger, M.T., Svrcek-Seilera, W.A., Flamm, C., Hofacker, I.L., Stadler, P.F., 2003. Efficient computation of RNA folding dynamics. *J. Phys. A* 37, 4731-4741.
- Xayaphoummine, A., Bucher, T., Thalmann, F., Isambert, H., 2003. Prediction and statistics of pseudoknots in RNA structures using exactly clustered stochastic simulations. *Proc. Natl. Acad. Sci.* 100, 15310-15315.

- Yang, G., Thompson, J.A., Fang, B., Liu, J., 2003. Silencing of H-ras gene expression by retrovirus-mediated siRNA decreases transformation efficiency and tumor growth in a model of human ovarian cancer. *Oncogene* 22, 5694-5701.
- Zamora, H., Luce, R., Biebricher, C.K., 1995. Design of artificial short-chained RNA species that are replicated by Q replicase. *Biochemistry* 34, 1261–1266.
- Zhang, W., Chen, S.J., 2002. RNA hairpin-folding kinetics. *Proc. Natl. Acad. Sci.* 99, 1931–1936.